

## A NEW HIGH-SENSITIVITY SUPERCONDUCTING RECEIVER FOR mm-WAVE REMOTE-SENSING SPECTROSCOPY OF THE STRATOSPHERE

*R.L. de Zafra, W.H. Mallison, M. Jaramillo\*, J.M.Reeves, L.K. Emmons, and D.T. Shindell*  
Physics Dept., State Univ. of N.Y.  
Stony Brook, N.Y., 11794.

\*(now at Univ. Javeriana-Cali, Colombia, S.A.)

**Abstract:** We describe a recently constructed ground-based mm-wave spectrometer incorporating a superconducting tunnel junction as a heterodyne mixer-receiver. Under conditions of low tropospheric water vapor, the superior sensitivity of this receiver allows spectral line measurements of stratospheric molecules with mixing ratios as small as a few tenths of a part per billion (e.g., ClO, HCN) to be made in 4 to 6 hours, with a signal to noise ratio of at least 30:1. We expect to be able to halve this time by further improvement of the mixer's intrinsic noise level.

Ground-based molecular emission-line spectroscopy is now a well-established method for obtaining stratospheric trace gas profiles and column densities. The earliest demonstrations of its technical feasibility occurred over two decades ago. The technique is still instrument-limited, however, and its sensitivity continues to improve with technical advances in detectors operating at mm-wave frequencies (~100 -300 GHz), a spectral region within which is found a large number of rotational emission lines from stratospheric trace gases. Intrinsic thermal emission noise from the stratosphere towards the upper end of this range is on the order of 100 K (given as an equivalent black-body emission temperature in the Rayleigh-Jeans limit). The best cryogenically cooled mm-wave detectors based on specially fabricated Schottky diode mixers typically have intrinsic noise temperatures of a couple of hundred degrees at 100 GHz, and 500-600 K at ~300 GHz. In these circumstances, the receiving equipment thus contributes substantially more than the atmosphere to the overall noise budget, and sets a practical limit to the detection of a number of interesting species.

Over the past decade, great progress has been made, primarily by the radio astronomy community, in exploring the use of superconducting tunnel junctions as heterodyne mixers, and in extending good performance to millimeter and sub-millimeter wavelengths. The structure of these junctions, a thin insulating layer sandwiched between two superconducting layers, has led to the nickname "SIS junction". In the past few years, several practical SIS based receivers have been put into sustained field use for radio astronomy. The noise temperatures available from present devices are significantly lower than those from any other type of coherent mm-wave detector. We have recently constructed a superconducting tunnel junction receiver to operate in the 260-280 GHz range for stratospheric spectroscopy\*, and report here on its design and present performance. This is the first mm-wave atmospheric spectrometer system to use this new technology.

SIS junctions are specially fabricated in a "handcraft industry". Our own are made by us at Stony Brook, using niobium as the superconductor and a thin aluminum oxide layer as a tunneling barrier. Two junctions are fabricated in close proximity on a quartz substrate, electrically connected in series to reduce effects of junction capacitance in shorting out high frequency signals. The active junction area is about 1 square micron. The junctions are electrically connected to a stripline IF choke structure, made along with the junctions by thin-film lithographic techniques. The quartz substrate measures 4 by 12 thousandths of an inch in cross section, and is about 1/4 inch long. The junctions are mounted within a waveguide measuring .0165 by .0330 inches in cross-section. The design of the mounting structure (i.e., mixer block) is very similar to that described by Ellison and Miller [1], scaled to a higher frequency range.

The use of Nb as the superconductor requires cooling to the 4 - 5 K range for good operation. In order to be free from transporting and storing large amounts of liquid helium to use as a coolant during extended field observations in isolated locations, we obtain cooling with a closed-cycle He refrigerator system [2]. This provides about 1/4 watt of cooling power at 4.5 K, sufficient for the detector and an ultra-low-noise preamplifier. A side-band filter termination (see below) is also cooled to a temperature of about 70 K. The refrigerator system is moderately bulky to transport, and consumes about 3.5 kW of electrical power, but provides a very stable operating temperature for many weeks at a time with little or no attention required.

Fig. 1 shows the overall physical and electronic layout of the receiver system. Conceptually, it is similar to an earlier Schottky diode-based receiver built at Stony Brook several years ago [3]. The SIS detector is mounted in a vacuum dewar, along with an ultra-low-noise preamplifier [4]. Both are cooled to about 4.5 K by the refrigerator. The SIS detector serves as a heterodyne down-converter, shifting the input spectrum (at present, tunable within the range ~260 - 280 GHz) down to an intermediate frequency (IF) centered at 1.39 GHz. The signal is then amplified by a factor of  $\sim 10^6$  and processed through an acousto-optic or filter-bank spectrometer. A standard theorem from optics makes it clear that signal intensity will not be increased with a larger collecting antenna, since an extended source (the sky) is being viewed. Thus, a small

\* This range can be changed, by substituting other heterodyne mixers and local oscillators, to cover the range from about 200-300 GHz using the present receiver system.

mm-wave feed horn would be sufficient as a collector. In practice, radiation from the stratosphere is guided to and focused at the feed horn by an off-axis parabolic mirrors of nominal 3 inch aperture (see Fig.1), creating in effect a 3 inch diameter collecting dish. This mirror also acts to reduce the acceptance angle of sky radiation to a cone with a half-angle of divergence equal to about 1.3 degrees. Modeling of the variation in signal intensity over the beam's "skyprint" shows that, to a very good approximation, the average signal intensity for a gaussian beam this small is that for a very thin 'pencil' beam pointing at the center of the true beam, down to an elevation angle of  $\sim 6^\circ$  above the horizon. A mirrored semicircular chopper wheel, rotating at about 1 Hz, alternately directs radiation to the detector from the zenith ("reference" direction) and from  $\sim 10$  degrees above the horizon ("signal" direction). A source of broad-band emission in the form of a relatively transparent dielectric sheet is placed in the reference beam to compensate for the weaker total power (spectral signal plus broadband background noise) radiated from the zenith direction. Residual variations from power balance (for instance, caused by time-varying atmospheric opacity) are removed by a servo system which adjusts the direction of the signal-beam viewing angle. Significant fluctuations in power at the detector for each spectral channel (primarily coming from the sky's broadband thermal emission) are thus virtually eliminated while alternating between viewing in the signal and reference directions. This helps to minimize instrumental artifacts in the spectral baseline.

We label the reference and signal directions R and S, respectively. The normalized difference spectrum  $[S(f)-R(f)]/R(f)$  is computed as a function of frequency  $f$  by data collection software for each rotation of the chopper wheel, and integrated over time. Due to the greater slant path length, an emission line appearing in the spectrum  $S(f)$  will have a greater intensity than in  $R(f)$ , and a net spectral signal will remain after the subtraction of  $S(f)-R(f)$ . Since the background of continuum radiation from the atmosphere, plus intrinsic noise from the heterodyne mixer, is a few hundred to several thousand times greater than trace-gas spectral features, division of the difference spectrum by  $R(f)$  merely serves to normalize the output, and does not impose any discernable spectral features on the difference spectrum.

The output  $[S(f)-R(f)]/R(f)$  is dimensionless. What we wish to recover as a standardized output is the spectral line shape and intensity, viewed in the zenith direction, as it would be recorded in the absence of the partially absorbing troposphere. (All emission lines considered here are optically thin, and self-absorption is negligible except for the strongest ozone lines.) Our method of determining tropospheric opacity and of recovering the desired zenith-looking spectrum from  $[S-R]/R$  is described in reference 3. Our method for calibrating the receiver sensitivity to establish an absolute scale for the emission line intensity as an equivalent black-body radiative temperature is also described there.

We have found that the SIS heterodyne mixer currently in use has rather different detection sensitivity in each of its two sidebands. This difference depends on tuning and the specific frequency range in use. It is technically difficult to accurately measure the relative or absolute response separately in each sideband of a heterodyne detector operating in the mm-wave frequency range, especially under field conditions. We have therefore added a tunable sideband filter, in the form of a polarizing interferometer [5], which suppresses response in the image sideband of the

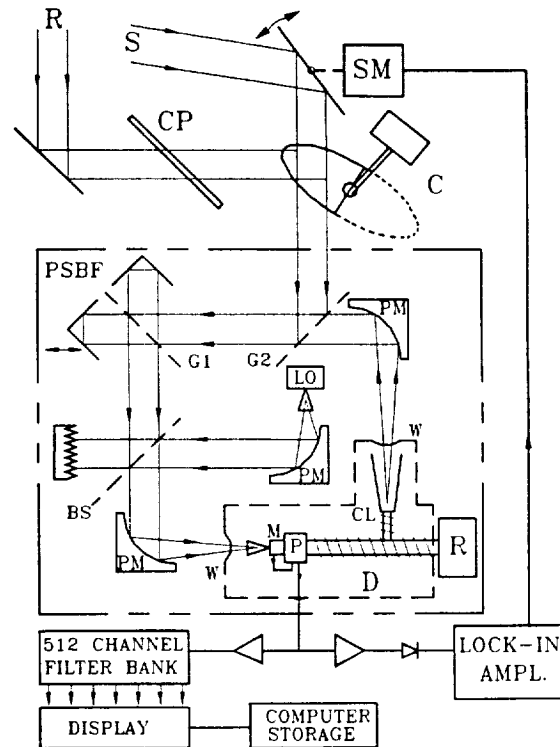
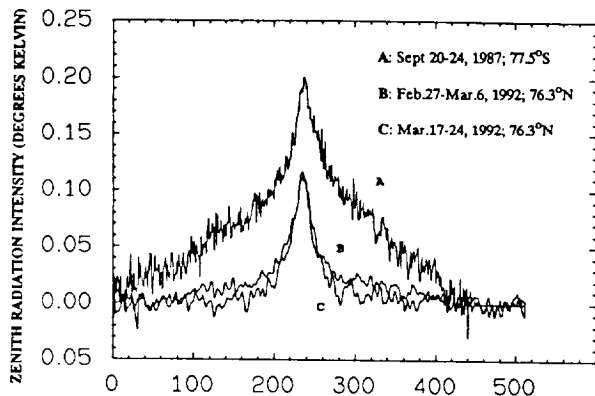


FIG.1: R,S = Reference and Signal directions; SM = servo mirror and motor; C = rotating chopping mirror; CP = Plexiglas power compensating plate; PSBF = polarizing side-band filter; G1, G2 = wire grid selective polarizers and reflectors; BS = 0.002" Mylar beam splitter; LO = local oscillator; PM = off-axis parabolic mirrors; M = SIS heterodyne mixer; P = preamp; R = cryogenic refrigerator; CL = terminating cold load for PSBF; D = vacuum dewar.

mixer. External hot and cold loads placed in the antenna beam can then be used to accurately calibrate the response in the remaining (signal) sideband [3]. The sideband filter has the added advantage of suppressing any spectral features from the image sideband which would otherwise be present in the spectrum. To lower the net noise temperature of the receiver, the image port for the sideband filter is terminated in an 80 K cold load, contained in the same dewar as the SIS detector.

The best noise temperature we have achieved is about 260 K under laboratory conditions, without the sideband filter. Under field conditions, with the sideband filter inserted, the receiver noise temperature has averaged about 360 K during a recent series of field measurements. This can and will be improved in the near future. It is already a factor of two better than the cryogenically cooled Schottky receiver used for our previous work [6]. Since the integrating time required to reach a given signal/noise level is proportional to the square of the total noise temperature (receiver plus atmosphere), this represents a significant improvement, reducing the required integration time to a few hours in the case of trace species like ClO, to achieve a signal to noise ratio of  $>30$  during reasonably good atmospheric conditions (opacity  $\sim .15$  in the zenith direction).



**Fig.3.** CIO emission lineshapes at Thule Greenland, vs McMurdo Station, Antarctica. Axes are as in Fig.2. The Mar 17-24, 1992 and Sept.20-24, 1987 spectra are at equal times following the winter solstice, and at ~equal latitudes. Strong line wings for Antarctic data are generated by a distinct low-altitude layer of high-density CIO. Slight line wings relative to Mar 17-24 are seen in the Feb 27-Mar 6 average. All data here is >4 hrs after sunrise and >4 hrs before sunset.

Deconvolution of the lineshapes for early February as well as for late March indicate no CIO below ~25 km with a mixing ratio >0.2 ppb (parts in  $10^9$ ), while the late February-early March data show some consistent evidence of an enhancement of CIO in the 20-30 km range, to values of ~0.5 ppb around 25 km. *We stress that this is far less than the 1-1.5 ppb value found consistently in a distinct layer peaking at ~20 km within the Antarctic vortex at an equivalent time of year [2,3,6], or in Arctic observations earlier in 1992 by UARS or the ER-2.*

It is also important to note that this weak low altitude enhancement does not represent 'stale' CIO entrained and spun off from the chemically processed inner vortex region to the periphery. Our observations of line-shape evolution from pre-dawn to post-sunset show it to be forming *in situ* on a daily basis, with a diurnal cycle of photo-driven growth and decay.

We believe this enhanced CIO may be forming as a result of chemical processing by stratospheric aerosols from Mt. Pinatubo, rather than as a result of 'conventional' polar stratospheric cloud processing. Certainly there seem to have been no PSC events in the Arctic during February or March<sup>[9]</sup>. A model by Atmospheric and Environmental Research, Inc.<sup>[10]</sup> shows that aerosol-induced enhancement is possible in an altitude range that qualitatively agrees with where we see enhanced CIO. The AER model with which we compare our data gives zonally averaged profiles, without regard for true meteorological transport in the Arctic. Its profile for Feb 15 at 76 N latitude shows a low altitude layer peaking at about 0.2 ppb at 22 km, certainly at the limit of our detection ability. The model gives a more general enhancement of CIO (by a factor of ~6 relative to a model involving only gas-phase chemistry) by mid-March within the entire stratosphere below ~30 km, though still <0.2 ppb anywhere below ~27 km, with a distinct lower layer no longer evident. The partitioning of Cl between HCl and CIO depends on methane concentration, which may not be correct for arctic conditions in this model, and might account for generally smaller CIO mixing ratios at

all altitudes than our deconvolutions generally yield. We intend to pursue a more thorough comparison between Arctic model predictions and our measurements in a later publication.

In a separate paper in these proceedings<sup>[11]</sup> we show that the stratosphere over Thule underwent a rapid change to higher levels of  $N_2O$  around March 8, when the circulation pattern changed, bringing air from the periphery of the Aleutian high over Thule for the first time. We presume that, in addition to carrying increased  $N_2O$ , this air restored stratospheric chemistry to conditions more typical of the normal non-polar stratosphere. It is not clear at this time whether this assumption is contrary to the Pinatubo aerosol processing discussed briefly above, since the latter should also affect non-Arctic stratospheric air, keeping CIO in an enhanced state in the 20-30 km range.

**Diurnal variation:** The diurnal variation of CIO that we observe in the polar stratosphere is markedly weaker than at low latitudes<sup>[5]</sup>. Fig.4 shows the diurnal change for data averaged over Feb 27-Mar 6. The series starts two hours before dawn at 40 km, and ends two hours after sunset. Spectra are averaged over two hour intervals counting forward from dawn and backwards from sunset. It is evident that there is relatively little change in peak line intensity throughout the diurnal cycle, and a particularly small change is apparent in both shape and intensity from the first two hours after sunset to dawn. (By Mar 6, the period between sunset and dawn is still ~11

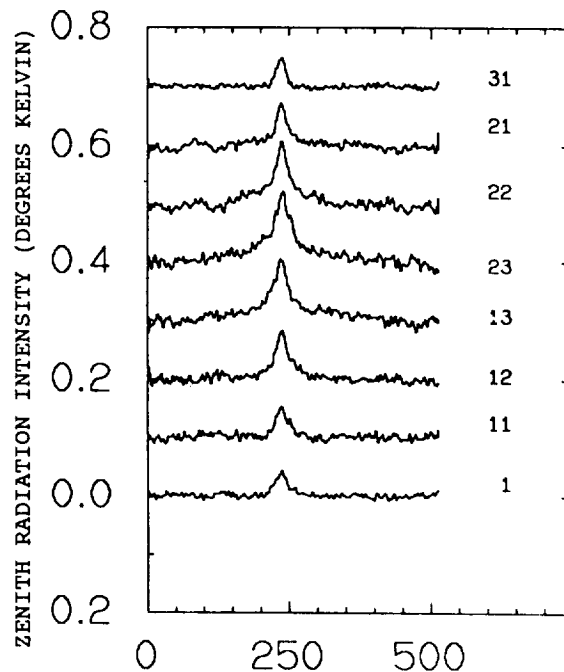


**Fig.4.** Diurnal variation for CIO emission data averaged over Feb 27-Mar 6. Axes are as in Fig.2. Trace 1 = 2-0 hrs before dawn at 40 km, 1N=successive 2-hour time averages counting forward from dawn; 2N = successive 2-hour averages counting backwards from sunset at 40 km; 31=0-2 hrs after sunset. Growth of weak line-wings is apparent in this data, but not in data of earlier February or late March.

hours.) The primary removal mechanism for ClO in the mid-stratospheric night is via combination with NO<sub>2</sub> to form ClONO<sub>2</sub>. Reaction with HO<sub>2</sub> to form HOCl is a second removal channel, dependent on the HO<sub>2</sub> mixing ratio with altitude. At 20° N latitude, these reactions decrease the total column of ClO above ~30 km by a factor of 10 from midday to the following dawn, for ~12 hours of darkness<sup>[5]</sup>. The very much smaller change evident in Fig. 4 (with total column proportional to integrated intensity) may be used as a proxy measure of NO<sub>2</sub> concentration (to the extent that removal of ClO by HO<sub>2</sub> is << than by NO<sub>2</sub>) in the Arctic middle stratosphere during the period in question. We note however, that even by late March, when other evidence points to a return of NO<sub>x</sub>-laden air to the Arctic over Thule, we still see surprisingly little day-night change. We plan to investigate this as part of a chemical model comparative analysis of our Thule data.

**Acknowledgements:** This work was supported by Grant NAGW-2182 from NASA's Upper Atmospheric Research Program and Grant NAG-1-1354 from the UARS Correlative Measurements Program. We greatly benefitted from meteorological and ozone data supplied by the Danish Meteorological Institute and the Norwegian Institute for Air Research, as part of our participation in the European Arctic Stratospheric Ozone Experiment of 1991-92. We also thank the Danish Polar Center and the U.S. Air Force for permission to use facilities at Thule Air Force Base, and for their cooperation during our stay.

#### References:

- [1]. R.L. de Zafra, W.H. Mallison, M. Jaramillo, J.M. Reeves, L.K. Emmons, and D.T. Shindell, "A New High-Sensitivity Superconducting Receiver for mm-wave Remote Sensing of the Stratosphere", these Proceedings.
- [2]. R.L. de Zafra, M. Jaramillo, A. Parrish, P. Solomon and J. Barrett, "High Concentrations of Chlorine Monoxide at Low Altitudes in the Antarctic Spring Stratosphere I: Diurnal Variation", *Nature*, **328**, 408-411, 1987.
- [3]. P.M. Solomon, B. Connor, R.L. de Zafra, A. Parrish, J. Barrett, and M. Jaramillo, "High Concentrations of Chlorine Monoxide at Low Altitudes in the Antarctic Spring Stratosphere II: Secular Variation", *Nature*, **328**, 411-413, 1987.
- [4]. L.T. Molina and M.J. Molina, "Production of Cl<sub>2</sub>O<sub>2</sub> from the Self Reaction of the ClO Radical", *J. Phys. Chem.* **91**, 433-436, 1987.
- [5]. P.M. Solomon, R.L. de Zafra, A. Parrish, and J.W. Barrett, "Diurnal Variation of Stratospheric Chlorine Monoxide: A Critical Test of Chlorine Chemistry in the Ozone Layer", *Science*, **224**, 1210-1214, 1984
- [6]. R.L. de Zafra, M. Jaramillo, J. Barrett, L.K. Emmons, P.M. Solomon, and A. Parrish, "New Observations of Large Concentrations of ClO in the Lower Springtime Stratosphere over Antarctica and Its Implications for Ozone-Depleting Chemistry", *J. Geophys. Res.*, **94**, 11423-11428, 1989, plus unpublished observations at McMurdo Station, September, 1991.
- [7]. Observations made during the European Arctic Stratospheric Ozone Experiment, (to be published).
- [8]. Unpublished data from the Second Airborne Arctic Stratospheric Expedition, and private communication from J. Waters for UARS measurements (to be published).
- [9]. Data from meteorological maps compiled by the Danish Meteorological Institute, and distributed through the Norwegian Institute for Air Research (NILU) during the EASOE campaign.
- [10]. Model output kindly supplied by J. Rodriguez, Atmospheric and Environmental Research, Inc., Cambridge, Mass. U.S.A. For partial description of this model, see J.M. Rodriguez, M.K.W. Ko, and N.D. Sze, *Nature*, **332**, 53-55, 1991.
- [11]. L.K. Emmons, J.M. Reeves, D.T. Shindell, and R.L. de Zafra, "Observed Changes in the Vertical Profile of Stratospheric Nitrous Oxide at Thule, Greenland, February-March, 1992", in these Proceedings.